Chapter 13

Quantification of Murine Pancreatic Tumors by High-Resolution Ultrasound

Stephen A. Sastra and Kenneth P. Olive

Abstract

Ultrasonography is a powerful imaging modality that enables noninvasive, real-time visualization of abdominal organs and tissues. This technology may be adapted for use in mice through the utilization of higher frequency transducers, allowing for extremely high-resolution imaging of the mouse pancreas. This technique is particularly well suited to pancreas imaging due to the ultrasonographic properties of the normal mouse pancreas, easily accessible imaging planes for the head and tail of the mouse pancreas, and the comparative difficulty in imaging the mouse pancreas with other technologies. A suite of measurement tools is available to characterize the normal and diseased states of tissues. Of particular utility for cancer applications is the ability to use tomography to construct a 3D tumor volume, enabling longitudinal imaging studies to track tumor development, or response to therapies.

Here, we describe a detailed method for performing high-resolution ultrasound to detect and measure pancreatic lesions in a genetically engineered mouse model of pancreatic ductal using the VisualSonics Vevo2100 High Resolution Ultrasound System. The method includes preparation of the animal for imaging, 2D and 3D image acquisition, and post-acquisition analysis of tumor volumes. The combined procedure has been utilized extensively by our group and others for the preclinical evaluation of novel therapeutic agents in the treatment of pancreatic ductal adenocarcinoma (Olive et al., Science 324:1457–1461, 2009; Cook et al., Methods Enzymol 439:73–85, 2008; Singh et al., Nat Biotechnol 28:585–593, 2010; Beatty et al., Science 331:1612–1616, 2011).

Key words: Ultrasound, Pancreatic ductal adenocarcinoma, Pancreas, Cancer, Mouse, Tumor quantification, Tomography

1. Introduction

Ultrasonography is a safe, noninvasive imaging modality that has found wide application in many areas of medical diagnostics, including obstetrics, cardiology, and oncology. However, it is perhaps underutilized in clinical oncology, and has only recently begun to

be utilized widely in the preclinical oncology setting. Ultrasonography is ideally suited to use in basic cancer research using small animal models since rapid, high-definition and reproducible tumor imaging can be made in vivo with only minor physiological impact on the subject. Accurate quantification of tumor volumes from this technique can provide detailed information on tumor growth kinetics, which is particularly important in fields such as preclinical therapeutics, where the response of tumors to therapies may be observed in real time.

Ultrasound imaging is based on the reflection of high-frequency sound by tissues. Sound pulses are emitted from a transducer held against the subject and the reflected signal is detected and used to construct an image. The physical principles underlying this technology are extensively reviewed elsewhere; this chapter focuses on the application of this technology to imaging the mouse abdominal cavity generally, and the pancreas specifically. From a practical standpoint, ultrasound can distinguish different tissues because each reflects greater or lesser proportions of the emitted signal. In general, fluid-filled tissues transmit more sound than air-filled tissues, and therefore the relative water content of tissues impacts the resulting image. For most soft tissues, as the sound passes through each point in the tissues, a fraction is reflected back to the tumor, while the rest continues on. As a result, tissues far away from the transducer (i.e., at the bottom of the screen for a linear array transducer) will appear darker or black. Furthermore, the transducer itself has an optimum focal depth where the best image is acquired (in some models this can be adjusted, while in others it is fixed).

Several other effects and artifacts may impact image quality. For example, air-filled tissues such as the stomach reflect most, or all, of the ultrasound signal. With the transducer applied from above, the top of the stomach will appear as a very bright (hyperechoic) rim, and underneath will be a black shadow. Shadowing occurs when all of the emitted sound is reflected leaving none to probe further into the tissue. This concept is illustrative both of the general principle of ultrasound imaging, and also of one of the chief difficulties: finding a clear window to view the organ of interest while avoiding opaque organs such as the stomach and air- or food-filled gut. The most common source of shadowing is from bubbles suspended in the gel that is placed between the transducer and the mouse's skin, which appear as small bright arcs with a dark cone beneath. The opposite of shadowing can also occur when a pocket of liquid, such as the bladder or a cyst, is surrounded by normal tissue. Comparatively less sound is reflected while traveling through the fluid than in surrounding tissues, resulting in a bright patch underneath the cyst, in an effect called "lensing." A final issue is the problem of bright bands that may occur from sound reflecting off the skin or the animal platform. Strategies for avoiding these artifacts are addressed below.

The techniques below are demonstrated using the KPC model of pancreatic ductal adenocarcinoma (PDA) (1). This genetically engineered model includes targeted mutations in K-ras and p53, two genes that are mutated in 90 and 75% of human pancreatic tumors (2, 3). The mutations are engineered in a conditionally inactive configuration, and their activation is restricted to pancreatic lineages through the activity of a Pdx1-driven Cre recombinase. Thus, K-ras$^{LSL.G12D/+}$; $p53^{R172H/+}$; PdxCre$^{tg/+}$ (KPC) mice develop a spectrum of premalignant lesions called pancreatic intraepithelial neoplasia (PanIN) that ultimately progress to ductal adenocarcinoma (1). Most KPC mice develop metastases in the liver, lungs, or peritoneum, the same sites where metastases are observed in human pancreatic cancer patients. The histopathology of the tumors that arise in the KPC model is very similar to that of human tumors (4) and they recapitulate the response of human tumors to chemotherapy and targeted therapeutics (5–7). As a result, the KPC model is becoming widely utilized for preclinical therapeutics studies (8).

High-resolution ultrasound is an excellent technology for imaging the tumors that arise in KPC mice (and related models). The ability to frequently and accurately monitor tumor volume over time provides invaluable information regarding the timing, extent, and duration of response to therapy. It should be noted that certain models of pancreatic cancer that have a very short survival time (for example, those with homozygous mutations in p53 or CDKN2A) can be more challenging to image because they develop a number of tumors throughout the pancreas that can be difficult to distinguish. KPC mice typically develop just one or two discrete tumors that in most cases can be readily imaged by ultrasound. However, based on the location of the tumor in the abdominal cavity, it can at times be challenging to distinguish the precise borders of the tumor in every frame of a 3D volume dataset. Thus it is critical that high-quality ultrasound data be acquired through the complete depth of the tumor to ensure accurate volumetric quantification.

2. Materials

All reagents directly injected into the subject animal must be sterile at the time of administration. Prepare and store all reagents at room temperature, unless otherwise stated.

2.1. Equipment

1. VisualSonics Vevo 2100 High Resolution System (see Note 1) with imaging stage, including dedicated anesthesia line and mouse nose cone.
2. VisualSonics Vevo 2100 3D motor, frame and mount.

3. Ultrasound transducer in the 25–55 MHz range, such as VisualSonics MS-550D (see Note 2).

4. Isoflurane anesthesia vaporizer/manifold with ability to supply at least three lines simultaneously (see Note 3), such as the RC^2 Rodent Anesthesia System from VetEquip.

5. Charcoal filters appropriate for isoflurane anesthesia waste gas scavenging (see Note 4).

6. Anesthesia induction chamber fitted with a waste-gas scavenging system.

7. Preparation mat: Heated or thermoregulated mat (see Note 5).

8. Handheld animal clippers with a fine blade.

9. Handheld vacuum cleaner.

10. Procedure room with workstations (see Note 6).

2.2. Reagents

1. Isoflurane (see Note 3).

2. Air or oxygen supply (see Note 7).

3. Depilatory cream: For example, Nair, Veet.

4. Phosphate-buffered saline (PBS): 10 mM sodium phosphate, 2 mM potassium phosphate, 2.7 mM KCl, 0.137 M NaCl, pH 7.2–7.4 (see Note 8).

5. Sterile normal saline for injection.

6. 70% Isopropanol (v/v) in deionized distilled water.

7. 70% Ethanol (v/v) in deionized distilled water.

8. Disinfectant spray: For example, T-Spray, Vimoba (see Note 9).

9. Ultrasound gel.

2.3. Consumables

1. C-fold paper towels.

2. Cotton tip applicators, e.g., Q-tips.

3. Gauze sponges.

4. Tissue wipes, e.g., Kimwipes.

5. 5 mL syringes.

6. 27 G needles.

3. Methods

All animal studies must be approved by relevant local and/or national authorities.

3.1. Animal Preparation

1. Switch on and initialize Vevo2100 System (see Note 1) as per manufacturer's instructions and prepare it for B-mode acquisition (see Note 10).

2. Fill a sealed anesthesia induction chamber with 2% isoflurane in air (or oxygen) through chamber for 2 min. Once charged, maintain anesthesia delivery of 1.5% isoflurane to all lines (induction chamber, preparatory station, imaging stage) when in use (see Note 3).

3. Place animal in induction chamber until animal shows no gross movement except for steady respiration. Confirm adequate anesthesia using the footpad reflex test (see Note 11).

4. Remove animal from induction chamber and stop flow of anesthesia to chamber. Move animal to preparatory station and start anesthesia flow to the station. Animal should be placed in a supine position on a dry paper towel covering a heated preparation mat with nose inside anesthesia line nose cone.

5. Using fine clippers, carefully shave fur from animal's ventral, lateral, and dorsal abdominal area, from hip joint to armpit (see Note 12). Use handheld vacuum cleaner to collect and remove shaved fur.

6. Apply a thin, even coat of depilatory cream to ventral and lateral shaved areas for 60–90 s. Using a folded gauze sponge dampened with neutral pH PBS, gently wipe treated area clean of depilatory cream and loosened fur. Spray treated area with excess PBS to neutralize any remaining depilatory preparation and pat dry with gauze sponge (see Note 13).

7. Place animal in prone position and repeat cream depilation of animal's shaved dorsal area.

8. Confirm that all depilatory cream has been completely removed from the animal's body.

9. Stop anesthesia flow to the preparatory station and start anesthesia to imaging stage. Move animal onto imaging stage, and place in supine position with nose inside anesthesia line nose cone.

10. Prepare a 4 mL delivery volume of saline, prewarmed to 37°C, in a 5 mL syringe with a 27 G needle attached (see Note 14).

11. Administer 4 mL of sterile saline by intraperitoneal injection (see Note 15).

3.2. Imaging

1. With animal in supine position, apply a generous layer of ultrasound gel over entire abdominal area. Aim to minimize trapped air bubbles between skin and gel and within gel itself (see Note 16).

2. Hold transducer in hand as one would hold a pen. Ensure that the notched side of the transducer is on the left for correct orientation of the image (see Note 17).

3. Place the transducer on the ultrasound gel above the abdomen and orthogonal to the plane of the imaging platform. Gently press down to visualize the internal organs (see Note 18).

4. Optimize image quality by adjusting transducer and display settings as per manufacturer's instructions (see Note 19).

5. Adjust the position of the mouse on the imaging stage (see Note 20) to minimize imaging artifacts such as reflection (see Note 21), shadowing (see Note 22), lensing (see Note 23), or distortions caused by bubbles in the ultrasound gel (see Note 24). Record this mouse position (see Note 25) (Fig. 1).

6. Identify pancreatic tissue (see Note 26) and abdominal "landmark" organs (see Note 27) that define specific regions of the pancreas (see Note 28) (Fig. 2).

7. Note the difference between "normal" and "diseased" pancreas, as well as any relevant tissue abnormalities such as cysts or ductal obstructions (see Note 29) (Fig. 2).

8. Locate any potential tumors within the pancreatic tissue (see Note 30) and adjust mouse position and image quality for optimal scanning throughout the entire tumor volume (see Note 31).

9. Clip the transducer onto the 3D motor attached to the motor frame and position onto the animal. By adjusting the coarse X- and Y-axis positions of the imaging stage, locate the tumor region to the center of the image display. Fine adjustment can then be made using the X- and Y-axis using the micrometer adjustors (see Note 32) (Fig. 3).

10. Using Y-axis adjustment, observe the tumor image quality from distal to proximal end and adjust as necessary. Note the end-to-end length of the mass and position the transducer at the midpoint.

11. Enable 3D image capture as per manufacturer's instructions. Ideally, a scan distance equal to the tumor length *plus* 4 mm is used, with a Z-slice thickness of 0.25 mm (see Note 33).

12. Review the images as collected during the 3D scan and note any artifacts or image distortions, including those due to animal movement (see Note 34). Repeat acquisition with remedial adjustments if necessary. Save the scan file and label appropriately with animal name, scan timepoint, tumor location, and mouse position.

13. If possible, reorient the animal's scanning position in order to obtain a second clear scan of the tumor (see Note 35). Save file and label appropriately.

14. Remove subject animal from imaging stage. Remove excess ultrasound gel from animal by gently swabbing with C-fold paper towels and/or gauze sponge. Return animal to cage on heated mat and monitor for recovery from anesthesia (see Note 36).

15. Remove excess ultrasound gel from all equipment with C-fold paper towels and/or KimWipes. Clean ultrasound transducer
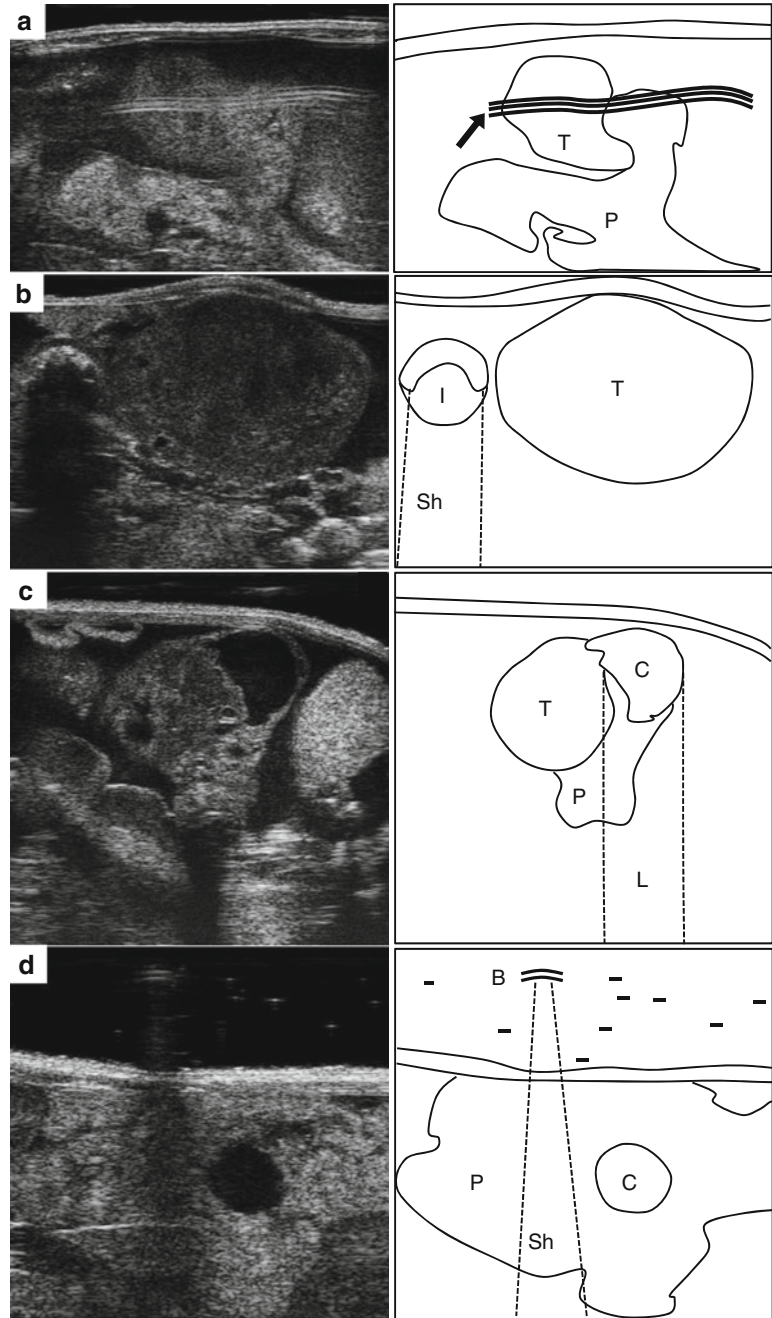
Fig. 1. Common ultrasound artifact. (**a**) Ultrasound image (*left*) of the tail of the pancreas, partially obscured by a reflection artifact. Map at right shows location of normal pancreas (P), a small pancreatic tumor (T), and reflection (*arrow*). (**b**) A large pancreatic tumor (T) is pictured next to a cross section of intestine (I). Note the *dark shadow* beneath the intestine (Sh). (**c**) A small, solid pancreatic tumor (T) is developing from a cystic lesion (C) in the tail of the pancreas (P). Note the bright region below the cystic lesion resulting from lensing. (**d**) Image of the pancreas tail (P) with a small cystic lesion (c). Small air bubbles (B) trapped in the ultrasound gel can produce shadows and distortions (Sh).
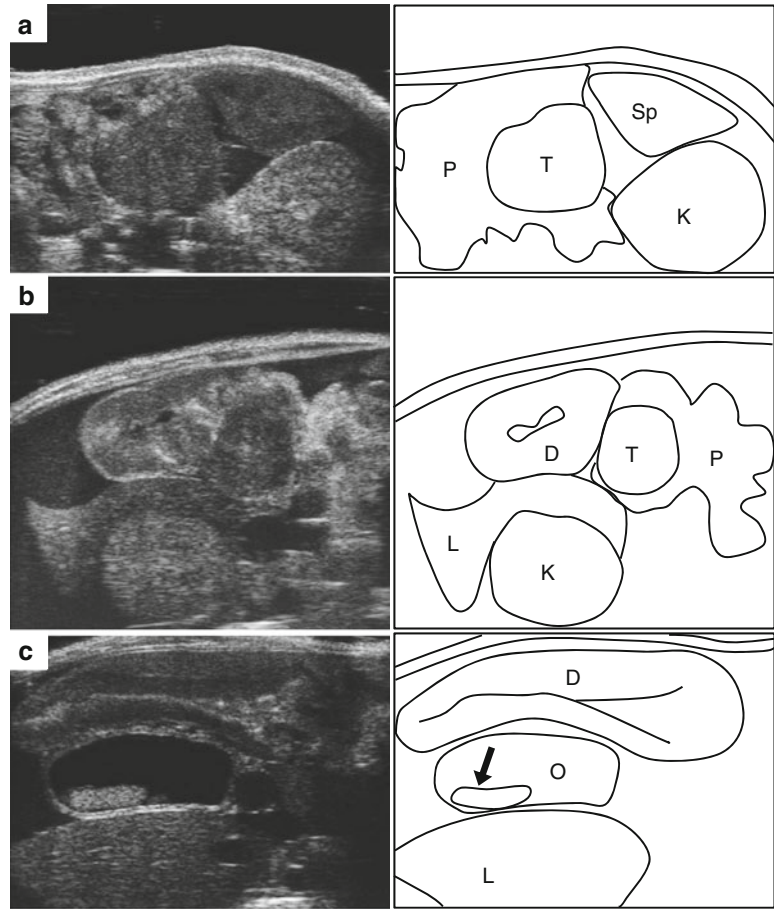
Fig. 2. Landmarks for location of the mouse pancreas. (**a**) Ultrasound image (*left*) of the tail of the pancreas (P), with a solid pancreatic tumor (T). Note location of the pancreas relative to the spleen (Sp) and left kidney (K). (**b**) The head of the pancreas (P) with a solid pancreatic tumor. This region can be more complicated to discern than the tail of pancreas. Landmarks include the proximal duodenum (D), which can be traced extending from the pylorus of the stomach. Also note the right kidney (K) and the right lobe of the liver (L). (**c**) Another common feature observed with head of pancreas tumors is the development of common bile duct obstructions (O). Here the bile duct is dramatically enlarged, and stones have developed (*arrow*). Nearby landmarks seen here include the duodenum (D) and the right lobe of the liver (L).

tip with 70% isopropanol. Clean imaging stage and anesthesia chamber with a noncorrosive disinfectant such as T-Spray. Clean preparation mats and benches with a suitable disinfectant such as Vimoba (see Note 4).

3.3. Post-acquisition Volumetric Analysis

1. Using the ultrasound software study management function, load the desired 3D scan file for analysis as per manufacturer's instructions.

2. Identify a Z-slice image in which the tumor/tissue border has the clearest definition.
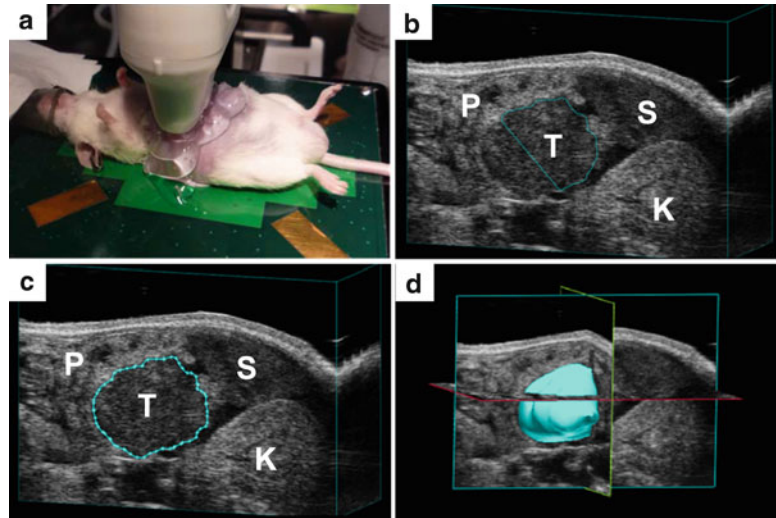
Fig. 3. Performing 3D ultrasound. (**a**) Experimental setup for imaging mice. (**b**) A tail of pancreas tumor (T) in the process of being quantified. Note spleen (S), left kidney (K), and surrounding pancreas (P). (**c**) A completed contour has been drawn around the tumor from B. (**d**) Once contours have been drawn around the tumor in each slice, the software can reconstruct a tumor volume and quantify the volume.

3. Initiate the volumetric analysis function and trace the tumor/ tissue border around the perimeter of the tumor, left-clicking to anchor specific points. When the entire border is traced, right-click to close the circle (see Note 37) (Fig. 3).

4. Proceed to add regions of interest (ROIs) on *every other* Z-slice through the depth of the tumor in both directions (see Note 38).

5. Complete the volumetric analysis function to derive final calculated tumor volume (see Note 39).

6. Once completed, the volume may be viewed as a framework or a solid surface, in the presence or the absence of the rest of the image. Multiple volumes may be defined on a single 3D dataset, and rendered in different colors.

4. Notes

1. This protocol presumes basic familiarity with the operation of a Vevo 2100 System consistent with the level of training provided by VisualSonics following purchase. Most of the techniques described here for image acquisition can be used with other suitable ultrasound instruments, such as the VisualSonics 770, although specific details regarding post-acquisition analysis may vary.

2. We find that 35 MHz is an ideal compromise between resolution and field of view for imaging pancreatic tumors. This frequency can provide a detailed view of small lesions while also allowing a complete view of all but the largest tumors. Certain applications require a larger field of view, or particular technical features such as nonlinear contrast, that are only available in lower frequency (13–24 MHz) transducers such as the VisualSonics MS-250.

3. Isoflurane is the preferred anesthetic agent for animal ultrasonography as it is easy to administer, responsive to dose control, generally well tolerated, and offers quick post-anesthesia recovery. Although the use of other anesthetic agents such as ketamine/xylazine is possible, their use is challenging in mice that are of varying performance status due to the systemic effects of pancreatic cancer. Tumor-bearing mice are often more sensitive to the effects of anesthesia and care should always be taken during the induction period of mice with tumors.

4. Waste gas scavenging can be performed using an active system that uses a vacuum to pull the excess anesthetic gas through a filter, or using a passive system that relies on the pressure from the small supply line to push the gas through a wider (and therefore lower pressure) tube leading to the charcoal filter. Active systems are more efficient at removing waste gas, but they require more space and careful balancing with the supply pressure. The risk of such active systems is that they can pull too much of the gas from the nose cone if not properly balanced, leading to difficulty in maintaining the plane of anesthesia.

5. Thermoregulated mats can often be sourced from a local pet shop for a small fraction of the cost that biomedical suppliers charge. An isoflurane line/nose cone can then be glued or taped to the pad to create a preparatory station separate from the ultrasound platform.

6. Establish four workstations at different places in the animal procedure room. The first station contains an induction chamber for anesthetizing the mice. The second station is set up for removing fur while maintaining body temperature and anesthesia. The third station is the ultrasound platform where the animal will be imaged. The fourth station is for post-procedure recovery and should include a recovery cage with clean bedding and a heating pad.

7. Either oxygen or air is appropriate for mixing with isoflurane during anesthesia. However, certain ultrasound contrast agents, including microbubbles, break down faster in mice breathing oxygen compared to air.

8. Preparation of a one-in-ten dilution of commercially available 10× PBS with deionized distilled water is sufficient for this purpose.

9. Ultrasound instruments present a significant risk of contamination for animal colonies because they are often used by multiple laboratories, then animals are taken out of microisolator cages, and fur is shaved making a significant mess. Therefore, decontamination and infection control is a major issue for all users. Your veterinary staff may recommend disinfectant sprays. Some disinfectants may be highly corrosive and these should not be used on the components of the ultrasound machine (such as the animal platform). Refer to manufacturer guidelines for effective noncorrosive disinfectants.

10. B-mode imaging is a two-dimensional composite image derived from an ultrasound transducer that displays a cross-sectional, real-time image.

11. Great care must be taken to monitor the well-being of the animal subject. During the procedure, mice must be kept on a heated mat or stage to maintain body temperature. Depth of anesthesia should be assessed regularly. Inadequate anesthesia dosing should be assessed by footpad reflex test (pinch the paw with your nail and watch for reflexive limb withdrawal). Slow respiration (<45 breaths/min), cyanosis (animal's muzzle appears blue), gasping, or other signs of respiratory distress may be signs of anesthetic overdose; to remedy, remove the animal from the nose cone until breathing has stabilized. The animal may then be returned to anesthesia, with reduced isoflurane content (percentage). Biometric monitoring by pulse oximetry may provide useful information on anesthesia status but may also interfere with optimal positioning of the animal for scanning.

12. Care must be taken when shaving the animal not to accidentally lacerate or graze the skin as depilatory cream should not be applied to open wounds. Mice with advanced tumors are often dehydrated and/or cachexic and this can make their skin loose and easily caught by clipper blades. In such cases, tighten the skin by stretching it over the abdomen with your fingers prior to shaving. Also, take extra care when shaving fur from the nipple line of female mice.

13. Depilatory cream is highly caustic and will cause chemical burns if applied for too long. Neutral pH PBS can neutralize the cream as soon as it is wiped from the animal's skin. A piece of gauze soaked in PBS will trap most of the excess cream. Flush the depilated area with copious volumes of PBS to thoroughly wash the skin. Please note that adjacent long fur may trap excess depilatory cream and should also be washed thoroughly.

We have found that damp medical gauze pads are more effective at removing depilatory cream than tissue wipes.

14. Air bubbles should be removed from the syringe prior to injection as air within the peritoneal space is ultrasonically opaque and will interfere with imaging.

15. The injection of 4 mL of sterile saline is very well tolerated by mice; the excess liquid is rapidly absorbed, and lost through urination within 24 h. We have performed this procedure on ~1,000 mice with no noticeable side effects. Nonetheless, this volume of i.p. injection is typically in excess of standard guidelines at many facilities. Therefore, it is critical to address this particular step when writing your IACUC (or similar animal authority) protocol.

Administer the IP injection via the animal's lower right abdominal quadrant. Insert the needle at a shallow angle (approximately 20–30°) to the skin surface about 5 mm into the abdomen. Prior to injection, gently attempt aspiration to ensure that the intestine (brown aspirate), bladder (yellow aspirate), or a blood vessel (red aspirate) has not been perforated. If any material is aspirated, dispose of the needle and syringe and replace; do not attempt to inject fecal, urinary, or blood material into the peritoneum as this can cause peritonitis.

16. A cushion of 3–8 mm depth of gel should be applied to the animal. This helps to space out the transducer from the skin and also provides an ultrasonically clear medium to conduct the sound waves into the animal. Air bubbles trapped within the ultrasound gel can interfere with good imaging. Although small bubbles may appear as no more than bright "stars" near the top of the image, larger bubbles may shadow tissue below them. In order to minimize this effect, apply the ultrasound gel directly onto the skin rather than pouring it from above, using liberal amounts. Extra gel can be dispensed in this way to "push" larger bubbles away from the ROI. Gel warmers or gel bottle centrifuges may assist to some degree with reducing bubbles in dispensing bottles. During prolonged scanning, it may be useful to apply additional gel if the image becomes less clear.

17. On the ultrasound, the top of the screen is closer to the transducer surface, and the bottom of the screen as further away. The left of the screen displays an image from the side of the transducer with the notch, and to the right is the opposite side. We will use up, down, left, and right to represent these four directions in this chapter. The transducer should be supported above the animal so that the cushion of gel is maintained. A common mistake is to press down on the animal with the transducer, which can make images less clear.

Rather, one should continually adjust the transducer up and down over the animal to find the distance that provides the clearest image.

18. Note any imaging artifacts caused by air bubbles or insufficient ultrasound gel and remedy as necessary by wiping the transducer tip and/or administering more gel. Take care not to press downward too firmly as this may distress or injure the animal; ideally, the abdomen should show only minimal outward distortion due to transducer pressure and the gel/skin border should be visible just below the depth offset point of the image.

19. Various imaging parameters may be adjusted to improve such image qualities as background noise signal, contrast between different organs or tissues, image resolution, and tumor/tissue border distinction. For example, *gain* adjusts the overall image brightness and may be increased to improve distinction of tissue borders or decreased to eliminate background noise. *Image depth* and *width* adjust the field of view and are useful for obtaining full visualization of ROIs while removing superfluous regions. *Focal depth* and *zone* adjust the depth and range over which beam focus and image quality are best and are ideally located at or slightly below the midpoint of the tumor image.

20. Positioning of the mouse is the single most important aspect of acquiring high-quality ultrasound images in the mouse abdomen. There are many possible sources of artifacts in an image, and patience can be necessary in cases where the tumor is obstructed. Be creative in trying as many different angles as possible to acquire the best image. It is advisable to acquire data from multiple angles for subsequent comparison.

21. Reflection artifacts are bright wavelike bands that can appear in the B-mode image. They are caused by reflection of the ultrasound signal from the gel, the animal's skin, or even from the image stage (Fig. 1a). They can often be minimized by slightly reducing the amount of gel, by cleaning and reapplying gel to the animal, or by slightly angling the transducer off orthogonal such that the signal beam reflects more away from the receiving transducer.

22. Shadowing artifacts occur when echo-dense structures shield areas of tissues below them, making them darker or invisible. Echo-dense structures include anything filled with air such as the stomach or intestines, or calcified tissue such as bone. It can obscure the border between tumor and normal tissues, or hide a small tumor entirely (Fig. 1b). Shadowing artifacts can be minimized by positioning the animal such that the tumor lies as close to the point of contact of the transducer as possible, without other overlaying tissue. In practice, this is

difficult to achieve, especially for "head of pancreas" tumors and so multiple imaging angles should be considered (see also Note 24).

23. Lensing artifacts may occur when the fluid in a cyst allows the ultrasound pulse to pass unimpeded through a column of space, compared to the surrounding tissues. This can result in a comparatively bright (hyperechoic) column below the cystic structure (Fig. 1c).

24. Bubbles suspended in the ultrasound gel between the transducer and the mouse can distort and shadow the image below. Warming the gel and/or centrifuging the ultrasound bottle may reduce the occurrence of bubbles, or they can be pushed aside manually with the transducer head.

25. In order to obtain the optimal quantifiable 3D image of the tumor, the animal should be positioned such that the border and mass remain as well defined as possible throughout the entire imaged volume. This may require rotating or angling the mouse and/or imaging platform to obtain the clear, unimpeded view required. Recording of the mouse position will assist in returning to the optimal imaging site and position for the subject animal at a later timepoint. We have defined "mouse position" based upon the rotational position of the animal on the imaging stage and the relative location of the mouse's tail on a clock. For example, when perfectly supine, the tail lies at the base of the mouse's transaxial perimeter (or, at "6 o'clock") and this is defined as mouse position 6 (MP6). Similarly, a perfectly prone mouse's tail lies at the top of the mouse's perimeter; thus we define this position "MP12." Animals positioned to lie on their right or left flanks are therefore at MP3 and MP9, respectively. Generally, "head of pancreas" tumors are best visualized in the range MP5 through MP11 while "tail of pancreas" tumors are best visualized in the range MP1 through MP7. Due to shadowing from the spinal column, MP12 is rarely used, but just offset from the spine (MP1 and MP11) can be very useful imaging positions for deep (dorsal) head of pancreas tumors. The imaging stage is also built on a ball and socket joint, which allows full rotation around the vertical axis (yaw if it were an airplane), and limited rotation around the lateral and longitudinal axes (pitch and roll, respectively). We rarely roll the platform along the longitudinal axis since the same effect is achieved by rotating the mouse. However, pitching the platform with the head up or down can be useful, and occasionally rotating yaw is useful as well. These positions should also be noted, for example, by P + 10 to indicate a 10° elevation in pitch (head up), and Y-45 to indicate 45° counterclockwise rotation. Thus a supine mouse with head up by 15° would be represented by "MP6, P + 15, Y0."

26. Healthy pancreas appears as smooth, bright (hyperechoic), homogenous tissue, and can be found in close association with the landmark organs described below. By easing the pressure of the ultrasound transducer on the animal, normal pancreas will be observed to float within the saline-filled peritoneum.

27. The kidney appears as a bright circular structure with a darker interior. The renal vein and artery are readily visible at their junction with the hilum of the kidney. The spleen is an oblate or slightly flattened structure of "mottled" (patchy dark and light) appearance (indicating red and white pulp). The stomach is a broad, ultrasonically opaque mass that shadows a large area, while the duodenum and intestinal loops appear circular or tubular, depending on their presented cross section. Small intestine tends to show a small lumen surrounded by a thick layer of villi, while large intestine has larger lumen and shorter villi. Intestinal loops may be variable in opacity and amount of shadowing they cast, depending upon the amount of food matter contained within.

28. From posterior to anterior, the tail of the pancreas is in direct proximity to the left kidney and spleen (Fig. 2b), the body lies close to the stomach and extends toward the pylorus, and the head resides anterior to the right kidney within the proximal loop of the duodenum and close to other intestinal loops (Fig. 2a). Occasionally, a posterior process of the pancreas can be detected extending from the head of the pancreas toward the right kidney.

29. Healthy pancreas has a smooth, bright, homogenous appearance on ultrasound (Fig. 2a). "Diseased" pancreas has a more mottled appearance than healthy tissue, with poorly differentiated bright and dark patches throughout (Fig. 2b). Often, the tissue takes on a denser, more rigid appearance that does not deform easily under gentle pressure from the transducer. Cystic structures can be identified as nearly spherical black regions with distinct borders surrounding them entirely. Since cysts are fluid filled, echoes from floating/settling sediment within these structures can give them a "snow globe" appearance. Similar to cysts, an obstructed common bile duct will also form large, spherical structures near the head of the pancreas (Fig. 2c). These are often distinguishable from cysts as having a visible epithelial layer surrounding the fluid-filled structure. Sedimentary material is also often seen within.

    Large cysts and obstructed ducts may act as conduits for sound, resulting in a column of brighter tissue below them. This effect is known as "lensing." It is rarely problematic for tumor detection or 3D imaging, but may complicate the quantification of contrast agents.

30. Pancreatic tumors can be identified as distinct, dark (hypoechoic), roughly spherical regions located within brighter normal or diseased pancreas. Generally, the border between the PDA and non-PDA regions is well defined. By easing the pressure of the ultrasound transducer on the animal, tumor masses often appear more rigid and retain their overall shape better than normal or diseased pancreas.

31. For the purposes of 3D tumor quantification, it is absolutely critical that the complete outline of the tumor is visible in every frame of the 3D image. The mouse should be repositioned repeatedly until the optimal position is identified that allows for the best possible 3D image.

32. Typically the transducer is mounted to provide an axial image and the motor scans the mouse posterior to anterior, though other orientations are possible.

33. When capturing a 3D image, consideration should be given to slice thickness and file size. The minimum possible step size is 0.05 mm. Smaller step sizes will give finer resolution but since the number of image frames is increased, the size of the whole 3D image file is also increased. For the purposes of volumetric quantification, the increase in resolution gained by very small step sizes is not matched by a comparable increase in quantification accuracy. We have chosen a step size of 0.25 mm as this is a reasonable compromise between resolution and file size.

34. Movement artifacts are distortions in a 3D scan caused by movement of the animal during the scanning process. "Dragging" occurs when the pressure applied by the transducer is large enough to drag the mouse along with the moving transducer as it takes the Z-slice scans. This is easily detected by monitoring the animal during the scan process. Respiration artifacts are caused by the natural displacement of abdominal organs associated with the breathing cycle. Often, sharp "jerks" can be seen in the Z-slices scanned as the animal draws a breath.

    It is possible to avoid respiration artifacts by employing respiratory gating. Briefly, the animal is connected to the imaging stage ECG monitor and its respiration wave is calculated. The program can then pause scanning and 3D motor progress during inhalation giving a much smoother 3D scan. Unfortunately, fastening the mouse to the ECG electrodes severely limits the operator's ability to manipulate the animal's position for optimal scanning (see Notes 20, 23, and 29) and can extend scanning time appreciably. Therefore, respiratory gating is not recommended for routine scanning; small respiration artifacts can be somewhat resolved by omitting the affected Z-slices during tumor quantification.

35. The elimination of all artifacts or interfering features from a 3D scan of pancreatic tumors is extremely difficult, so obtaining multiple scans of the same tumor from different angles is recommended. This allows for a better appreciation of the tumor's overall shape and location, thus clarifying less distinct tumor areas or borders seen in one scan only.

    Multiple scans also allow for comparative volumetric analyses to be performed. Since only the scanning angle has been changed, volume quantification of each scan should yield the same result as long as consistent application of "ROI" definition is made.

36. The mouse should regain consciousness within a few minutes of being removed from isoflurane, and should start walking shortly thereafter. Prolonged recovery time may indicate a mouse that is not well. Such animals should be monitored extensively. Once awake, the mouse may be returned to its cage, ideally with other mice that will help keep the mouse warm. On the day after ultrasound, mice should be observed to confirm that the i.p. saline has been absorbed. If an animal still appears bloated with abdominal fluid, after 24 h, it must be euthanized rapidly as it will not recover (when mice develop abdominal ascites they lose the ability to absorb injected saline).

37. Fine editing of the traced ROI is possible by moving the individual points that define the ROI. In general, small modifications lead to very small changes in overall calculated volume.

    ROI border definition is entirely reliant upon image quality for discrimination of the tumor/tissue border. Unfortunately, areas often appear within individual Z-slice images where this distinction is difficult or poor. This can be due to local artifacts or distortions that can be impossible to entirely remove from a 3D scan. In these cases, a rapid scrolling through the 3D volume can give insight into the correct location of this border. The viewer's ability to recognize the pattern of border placement using adjacent slices allows one to discern edges that are impossible to pick out from a single image. For this reason, manual annotation of 3D volumes is still far superior to even the best-automated algorithms.

    By nature, there is a subjective component to ROI border definition. Therefore, if multiple users are to produce comparable volumetric analyses, consistency in their methods must be ensured. This is best achieved by independent, blinded analysis by the users of a set of 3D scans, followed by a detailed examination and discussion of significant areas of specific and general difference in each user's ROI definitions. This can help create a consensus regarding the definition of ROIs, leading to a more uniform application of the technique.

38. The number of Z-slices per ROI required for accurate volumetric quantification is dependent upon the step size. For a slice thickness of 0.25 mm, ROI tracing of every second slice is regarded as sufficient. While one could achieve the same resolution using a step size of 0.5 mm, the additional slices provide useful information when the border is indistinct, when respiration artifact causes one frame to be unusable, or when the tumor rapidly changes size. The 3D quantification software extrapolates the volume of the missing slices based on those on either side.

39. When multiple tumor volumes are acquired over time (longitudinal imaging), we advise performing 3D quantification of all tumors in one session post hoc. This allows for the greatest level of consistency in how a tumor was measured from point to point. When performing drug studies, by convention we set the day on which the animal received the first treatment to be Day 0.

References

1. Hingorani SR et al (2005) Trp53R172H and KrasG12D cooperate to promote chromosomal instability and widely metastatic pancreatic ductal adenocarcinoma in mice. Cancer Cell 7:469–483

2. Hruban RH et al (1998) Tumor-suppressor genes in pancreatic cancer. J Hepatobiliary Pancreat Surg 5:383–391

3. Hruban RH et al (1993) K-ras oncogene activation in adenocarcinoma of the human pancreas. A study of 82 carcinomas using a combination of mutant-enriched polymerase chain reaction analysis and allele-specific oligonucleotide hybridization. Am J Pathol 143:545–554

4. Hruban RH et al (2006) Pathology of genetically engineered mouse models of pancreatic exocrine cancer: consensus report and recommendations. Cancer Res 66:95–106

5. Olive KP et al (2009) Inhibition of Hedgehog signaling enhances delivery of chemotherapy in a mouse model of pancreatic cancer. Science 324:1457–1461

6. Singh M et al (2010) Assessing therapeutic responses in Kras mutant cancers using genetically engineered mouse models. Nat Biotechnol 28:585–593

7. Beatty GL et al (2011) CD40 agonists alter tumor stroma and show efficacy against pancreatic carcinoma in mice and humans. Science 331:1612–1616

8. Cook N et al (2008) K-ras-driven pancreatic cancer mouse model for anticancer inhibitor analyses. Methods Enzymol 439:73–85